Thomas, K. A. Baglan, N. C., & Bradshaw, R. A. (1981) *J. Biol. Chem. 256*, 9156–9166.
van Leeuwen, B. H., Evans, B. A., Tregear, G. W., & Richards, R. I. (1986) *J. Biol. Chem. 261*, 5529–5535.
Wallace, L. J., & Partlow, L. M. (1976) *Proc. Natl. Acad. Sci. U.S.A. 73*, 4210–4214.
Wilson, W. H., & Shooter, E. M. (1979) *J. Biol. Chem. 254*, 6002–6009.

# Rotational Dynamics of the $Fc_\epsilon$ Receptor on Mast Cells Monitored by Specific Monoclonal Antibodies and IgE†

Israel Pecht,*,‡ Enrique Ortega,‡ and Thomas M. Jovin*,§

*Department of Chemical Immunology, The Weizmann Institute of Science, Rehovot 76100, Israel, and Department of Molecular Biology, Max Planck Institute for Biophysical Chemistry, 3400 Göttingen, Federal Republic of Germany*

*Received April 20, 1990; Revised Manuscript Received September 28, 1990*

ABSTRACT: The rotational motions of the type I receptor for the $Fc_\epsilon$ domains ($Fc_\epsilon RI$) present on mast cells were investigated by measuring the phosphorescence emission and anisotropy decay kinetics of erythrosin (Er) covalently bound to several $Fc_\epsilon RI$-specific macromolecular ligands. The latter consisted of three murine monoclonal antibodies (IgG class) raised against the $Fc_\epsilon RI$ of rat mast cells (RBL-2H3 line), their Fab fragments, and a murine monoclonal IgE. Different anisotropy decay patterns were observed for the three monovalent Er–Fab fragments bound to the $Fc_\epsilon RI$, reflecting the rotational motion of the $Fe_\epsilon RI$ reported by each specific macromolecular probe bound to its particular epitope. Internal motions of the tethered Er-labeled ligands may also contribute to the observed anisotropy decay, particularly in the case of cell-bound IgE. The results corroborate an earlier study with rat Er–IgE in which the $Fc_\epsilon RI$–IgE complex was shown to be mobile throughout the temperature range examined (5–37 °C). The anisotropy decays of the three Er-labeled, $Fc_\epsilon RI$-specific intact mAbs bound to cells also differed markedly. Whereas the decay curves of one mAb (H10) were characterized by temperature-dependent positive amplitudes and rather short rotational correlation times, the decay of a second mAb (J17) showed complex qualitative variations with temperature, and in the case of the third antibody (F4), there was no apparent decay of anisotropy over the time and temperature ranges examined. The spectrum of rotational mobility data obtained for the complexes of the $Fc_\epsilon RI$ with the mAbs and their Fab fragments is consistent with the suggestion that the orientations of the antibody probes with respect to the $Fc_\epsilon$ receptor, and thus to the cell membrane, are nonrandom and different. This feature may be decisive in the $Fc_\epsilon RI$-cross-linking process induced by each of the mAbs and in the resulting cellular response culminating in exocytosis. A possible inverse correlation between the rate of rotational depolarization of a given Er–mAb cross-linking $Fc_\epsilon RI$ and its secretion-inducing capacity can be proposed.

The type I receptor for $Fc_\epsilon$ domains of IgE ($Fc_\epsilon RI$)[1] is an integral plasma membrane complex of four polypeptide chains present only in mast cells and basophils (Froese, 1984; Metzger et al., 1986; Kinet, 1989). The minimal $Fc_\epsilon RI$ unit is thought to be a complex ($\alpha\beta\gamma_2$) of one $\alpha$ chain (50 kDa), one $\beta$ chain (35 kDa), and a disulfide-linked $\gamma$ chain dimer (14 kDa) (Blank et al., 1989; Metzger et al., 1986). $Fc_\epsilon RI$ binds a single IgE molecule primarily via its $C_\epsilon 3$ domain, although the $C_\epsilon 2$ and $C_\epsilon 4$ domains are also involved (Helm et al., 1988; Schwarzbaum et al., 1989). The $\beta$ and $\gamma$ polypeptide chains are associated noncovalently with the IgE-binding $\alpha$ subunit and are therefore coisolated from mast cell (RBL-2H3 line) membranes in an affinity-based purification process (Rivnay et al., 1982). No biochemical or biological effects can be detected following the monovalent binding of IgE to $Fc_\epsilon RI$ on the cell surface. Hence this step may be regarded as the priming process of the system, endowing it with antigen-binding specificity corresponding to the variable regions of the IgE. It is the clustering of the $Fc_\epsilon RI$, induced either directly by specific antibodies or via the bound IgE by specific polyvalent antigens or anti-IgE antibodies, that provides the signal initiating the cascade of processes culminating in mediator secretion (Ishizaka & Ishizaka, 1984). A number of biochemical processes have been observed following $Fc_\epsilon RI$ aggregation that are assumed to constitute the cascade coupling this stimulus to secretion. However, the actual involvement and temporal sequence of these steps in the overall mechanism are not clearly resolved and constitute topics of major research activity (Ishizaka & Ishizaka, 1984; Metzger et al., 1986; Siraganian, 1988).

Plasma membrane receptor clustering as the initial step of a cellular stimulus is a general phenomenon observed for a diversity of signaling mechanisms in mammalian cells (De Lisi, 1979). In particular, immunological stimuli are characterized by a requirement for receptor aggregation, as illustrated by different types of antigen–receptors cross-linked by multiple

† Financial support was generously provided by grants from The M. and J. Heinemann Foundation and from The Thyssen Foundation, FRG.
* To whom correspondence should be addressed.
‡ The Weizmann Institute of Science.
§ Max Planck Institute for Biophysical Chemistry.

[1] Abbreviations: $Fc_\epsilon RI$, type I receptor for $Fc_\epsilon$ domains; RBL-2H3, rat basophilic leukemia cells, subline 2H3; Er, erythrosin (tetraiodofluorescein); mAb, monoclonal antibody; DNP, 2,4-dinitrophenyl; FCS, fetal calf serum; PBS, phosphate-buffered saline (137 mM NaCl, 2.7 mM KCl, 8.4 mM sodium/potassium phosphate, pH 7.2).

0006-2960/91/0430-3450$02.50/0 

interactions with specific polyvalent ligands. As a consequence, the mobility and state of aggregation of cell surface receptors are important properties. They can be monitored experimentally by measurements of lateral and rotational diffusion (Edidin, 1987; Jovin & Vaz, 1989). The lateral mobility of $Fc_\epsilon RI$ on mast cells (RBL-2H3 line) was recently reinvestigated by monitoring cell-bound, fluorescently labeled IgE. While no effect of the bound IgE on receptor mobility could be discerned (McCloskey et al., 1984), different protocols of IgE cross-linking were found to immobilize the receptors in a process that could not be rationalized by simple hydrodynamic considerations (Menon et al., 1986a,b). Time-resolved phosphorescence anisotropy decay is an appropriate and sensitive method for measuring the rotational dynamics of membrane components labeled with suitable triplet probes, the lifetimes of which lie in the microsecond to millisecond range expected for motions of macromolecules embedded in the viscous plasma membrane. The time course of phosphorescence anisotropy has been shown to reflect directly the size and mobility of the labeled membrane component and hence its state of aggregation (Zidovetzki et al., 1986a,b; Jovin & Vaz, 1989). The rotational dynamics of Er–IgE bound to the $Fc_\epsilon RI$ on living mast cells has been previously studied by time-resolved phosphorescence emission and anisotropy (Zidovetzki et al., 1986b; G. Barisas, I. Pecht, and T. M. Jovin, unpublished data).

Monoclonal antibodies (mAbs) specific for cell-membrane receptors have been widely employed for the isolation, probing, and modulation of the respective antigens. We have recently raised several mAbs specific for the $\alpha$ chain of $Fc_\epsilon RI$ and demonstrated that they are very useful reagents for the quantitative analysis of receptor aggregation and the secretory stimulus thereby provided to the mast cells (Ortega et al., 1988). Three such mAbs were shown to have a binding stoichiometry of one Fab per $Fc_\epsilon RI$. Since the mAbs are of the IgG class, they are capable of cross-linking the receptors only into dimers. Nonetheless, the mAbs induce mediator secretion from mucosal mast cells of the rat cell line RBL-2H3, clearly showing that formation of an initial aggregate of this minimal size is sufficient for producing the secretory signal even in this type of mast cell. The intrinsic affinities of the Fab fragments derived from each of the mAbs as well as the binding constants of the intact antibodies have been determined. By use of IgE binding to determine the number of $Fc_\epsilon RI$ per cell, the extent of receptor dimerization attained with each of the mAbs was computed but shown not to correlate simply with the cellular secretory response. Hence, it was proposed that the differences result from distinct orientational constraints imposed by each different mAb on the $Fc_\epsilon RI$ upon dimerization (Ortega et al., 1988).

The three mAbs as well as their Fab fragments have been employed in this work for studying the motional dynamics of the $Fc_\epsilon RI$ in the plasma membranes of live RBL-2H3 cells. Measurements of the anisotropy decay kinetics of phosphorescence emitted by erythrosin (Er) covalently bound to the ligand proteins were performed. We studied the $Fc_\epsilon RI$ mobility and state of aggregation, first with the cell-bound monovalent Fab fragments and IgE, and then with the intact mAbs following binding to and cross-linking of the $Fc_\epsilon RI$ on the cell surface.

## Materials and Methods

*Reagents.* Erythrosin-5′-isothiocyanate was purchased from Molecular Probes, Eugene, OR. Sepharose 4B, Sepharose–protein A, and Sephadex G-25 were from Pharmacia, Uppsala, Sweden. DNP–Sepharose was prepared by reacting $N^\epsilon$-(2,4-dinitrophenyl)lysine with CNBr-activated Sepharose 4B. All salts and other reagents were of the highest purity available.

*Monoclonal Antibodies.* The mAbs F4, J17, and H10 were purified from culture supernatants by chromatography on protein A–Sepharose as previously described (Ortega et al., 1988). Fab fragments of these were prepared by papain digestion as described in the above reference. DNP-specific mouse IgE (produced by the hybridoma line 26.82; Liu et al., 1980) was affinity-purified from ascites fluid by chromatography on DNP–sepharose (Goetzl & Metzger, 1970). Labeling of the purified proteins with erythrosin-5′-isothiocyanate was carried out for 2 h at room temperature, pH 8, in the dark, with a dye/protein ratio of 6. Unreacted dye was separated by gel filtration on 10-mL columns of Sephadex G-25. For determination of the degree of labeling, an $\epsilon^{540nm} = 83\ mM^{-1}\ cm^{-1}$ for erythrosin was used. The erythrosin/protein ratios obtained were F4 mAb,1.5; F4 Fab, 1.8; H10 mAb, 0.44; H10 Fab, ~0.1; J17 mAb, 0.7; J17 Fab, 0.2; and IgE, ~2.

*Cell Preparations.* RBL-2H3 cells were grown as subconfluent cultures in Dulbecco's-modified Eagle's medium (DMEM) supplemented with 10% FCS. Cells were harvested by short incubation with Tris–saline containing 20 mM EDTA. After being washed and counted, the cells were resuspended to $(2–3) \times 10^7$ cells $mL^{-1}$ in DMEM with 0.5 mg $mL^{-1}$ BSA. Binding of the Er-labeled ligands (IgE, the mAbs, or their Fabs) was carried out by incubation with the respective ligand at equivalent or slight excess over the $Fc_\epsilon RI$ concentrations for 1 h at 0 °C, with occasional shaking. After being washed, the cells were resuspended in PBS (0.87 mM $Ca^{2+}$ and 0.5 mM $Mg^{2+}$) at a density of $(1–2) \times 10^7$ cells $mL^{-1}$.

*Time-Resolved Phosphorescence Measurements.* The principles of the instrumentation and methods for determination of time-resolved phosphorescence and anisotropy decay have been described previously (Matayoshi et al., 1983; Zidovetzki et al., 1981, 1986a,b; Jovin & Vaz, 1989). Excitation of the erythrosin-labeled reagents was with a ~10-ns, 1–3-mJ, vertically polarized pulse (514 nm) generated by an excimer laser (EMG 50, Lambda Physik, Göttingen, FRG) pumping a FL2000 dye laser (Lambda Physik) at 308 nm; the dye was Coumarin 307. The cell suspensions [$(\sim 1–2) \times 10^7$ cells $mL^{-1}$] were placed in 5 × 5 mm quartz cuvettes and freed from $O_2$ by plunger action under a constant stream of dry argon or, alternatively, by enzymatic means. The latter was achieved by the combined activity of glucose oxidase and catalase (final concentrations 0.025 and 0.015 mg $mL^{-1}$, respectively) and glucose (25–50 mM) as the substrate. The thermostated cuvettes were irradiated at a frequency of ~10 Hz, and the polarized phosphorescence was measured through a train of optical filters: 2 mm of saturated potassium dichromate in $H_2O$, a KV550 barrier filter (Schott, Mainz, FRG), a rotating film polarizer, a KV550 filter (Schott), and a RG645 barrier filter (Schott). The detector was an EMI 9816QGA photomultiplier gated electronically so as to suppress the prompt fluorescence coincident with the excitation pulse (Yashida et al., 1989). In general, records of 1000 decay curves for both emission polarization components (measured in alternation, each with 50 pulses at a time) were accumulated. These files were either analyzed individually or as sums of 3–5 files so as to reduce the statistical noise component. Results of these analyses are reported in the figures and tables. The total emission functions $S(t)$ and the anisotropy decay $r(t)$ curves were formed from the parallel and perpendicular polarized components, $I_\parallel$ and $I_\perp$, respectively.

$$S(t) = I_\parallel + 2I_\perp \quad (1)$$

$$r(t) = (I_{\parallel} - 2I_{\perp})/(I_{\parallel} + 2I_{\perp}) \quad (2)$$

The correction factors reported previously (Jovin & Vaz, 1989) were not required in the present optical configuration. The $S(t)$ curves were analyzed by a nonlinear least-squares algorithm for two or three exponential components (with lifetimes $\tau_i$). The analytical curves were then used to generate weighting factors $[S(t)^2]$ in the analysis of the corresponding $r(t)$ curves, usually represented as the sum of an exponential decay and a limiting anisotropy, the analysis of which involves estimation of three parameters

$$r(t) = \alpha \exp(-t/\phi) + r_{\infty} \quad (3)$$

in which the time constant $\phi$ (the rotational correlation time) is an inverse function of the diffusion constant(s) and thus a measure of rotational, wobbling, and segmental motions of the probe and the macromolecular carrier to which it is conjugated (Lipari & Szabo, 1980; Szabo, 1984; Kinosita et al., 1984). The initial anisotropy $r_{in}$ is calculated as the sum of the decay amplitude $\alpha$ and the limiting anisotropy $r_{\infty}$. The latter reflects the anisotropic equilibrium distribution of the probe(s) after rotational depolarization. In some cases, a two-component analysis was required for a satisfactory fit of the data. All measurements were carried out as a function of temperature according to the protocols indicated in the previous section.

*Anisotropy of Erythrosin–mABs in High-Viscosity Medium.* Erythrosin-labeled mAbs and Fab fragments were diluted to the required concentration by addition to an aqueous sucrose solution. To 800 μL of ~70% (w/w) sucrose were added 5–10 μL of labeled probe, 10 μL of 0.5 M glucose, and 10 μL of the oxygen-scavenging enzymes (glucose oxidase 0.5 mg $mL^{-1}$, catalase 0.3 mg $mL^{-1}$). [In this medium, adequate triplet lifetimes were also obtained without enzymatic deoxygenation.] The samples were mixed to homogeneity and filled into carefully dried cuvettes. Aliquots of each sample were taken for refractive index measurements at 21 °C, yielding the sucrose concentrations required for calculation of solution viscosities at the different temperatures (Kaganov, 1982).

## Results and Discussion

Aqueous buffer solutions of erythrosin conjugates of the three different mAbs, of their respective Fab fragments, and of the monoclonal IgE exhibited a characteristic phosphorescence emission that decayed in the microsecond to millisecond time domain.

*Anisotropy Decay of Er-Labeled Conjugates in High-Viscosity Medium.* The phosphorescence anisotropy decay kinetics of both Er–mAbs and the Er–Fabs were measured in viscous solutions (~70% sucrose in water) in order to assess the extent of emission depolarization caused by fast motions of the Er probe itself and by segmental flexibility of the mAb or its Fab fragment. The anisotropy decay parameters of Er conjugated to the intact mAbs and the Fab fragments dissolved in sucrose solutions are summarized in Table I, and a set of illustrative decay curves are presented in Figure 1. All three Er–Fab derivatives exhibited positive anisotropy decay curves that differed significantly from those observed with the same ligands bound to the $Fc_{\epsilon}RI$ on RBL-2H3 cells (see below). The initial anisotropies, $r_{in}$, of the Er–Fabs were in the range 0.08–0.11, values similar to those for the conjugated monoclonal IgE. In some cases (Table I), the final anisotropies, $r_{\infty}$, were significantly greater than zero, the value expected for rotational depolarization in an isotropic medium. We attribute those findings to the generation of antibody aggregates upon dilution with concentrated sucrose solutions; this problem was particularly severe with the Er–IgE. The rotational correlation times scaled to the viscosity of water were internally consistent and in the expected order IgE > mAb > Fab. The values also

Table I: Phosphorescence Anisotropy Decay Parameters for Erythrosin Conjugates of IgE and $Fc_{\epsilon}RI$-Specific Antibodies in High-Viscosity Solutions (~70% Sucrose)

| protein | $T$ (°C) | $\phi$ (μs) | $\alpha$ | $r_{\infty}$ | $r_{in}$ | $\eta^a$ (cP) | $\phi^b$ (ns) |
|---|---|---|---|---|---|---|---|
| IgE | 22 | 79[c] | 0.080 | 0.024 | 0.104 | 200 | 390[c] |
| H10 Fab | 7 | 22 | 0.083 | 0.016 | 0.099 | 580 | 36 |
| J17 Fab | 7 | 40 | 0.126 | −0.002 | 0.124 | 1250 | 30 |
| | 16 | 18 | 0.109 | −0.001 | 0.108 | 470 | 37 |
| F4 Fab[d] | 7 | 59 | 0.093 | −0.006 | 0.087 | | |
| H10 mAb | 16 | 50 | 0.090 | 0.010 | 0.100 | 410 | 118 |
| | 23 | 35 | 0.080 | 0.015 | 0.095 | 240 | 145 |
| J17 mAb | 16 | 47 | 0.089 | 0.003 | 0.092 | 410 | 107 |
| | 23 | 32 | 0.082 | 0.004 | 0.086 | 240 | 132 |
| F4 mAb | 16 | 49 | 0.085 | 0.000 | 0.085 | 400 | 119 |
| | 23 | 33 | 0.079 | −0.001 | 0.078 | 240 | 137 |

[a] Viscosity was calculated from the measured refractive index to obtain sucrose concentration and from a parametric equation for the viscosity of sucrose solutions as a function of concentration and temperature [eq 5 in Kaganov (1982)]. The sucrose concentrations were in the range 65.8–68.6% (w/w). [b] Rotational correlation time was normalized to 25 °C and 1 cP ($H_2O$) by multiplication by the factor $(T/298)\eta$ with $T$, the absolute temperature. [c] This value is probably too high due to the distorting effect of aggregated IgE. [d] In this (and other measurements), the indicated parameters were calculated from a file generated by averaging the raw data from three records. In analyzing the latter individually, the ranges of values for $\phi$, $\alpha$, and $r_{in}$ (expressed as percentages of the means) were 14, 2, and 5, respectively.

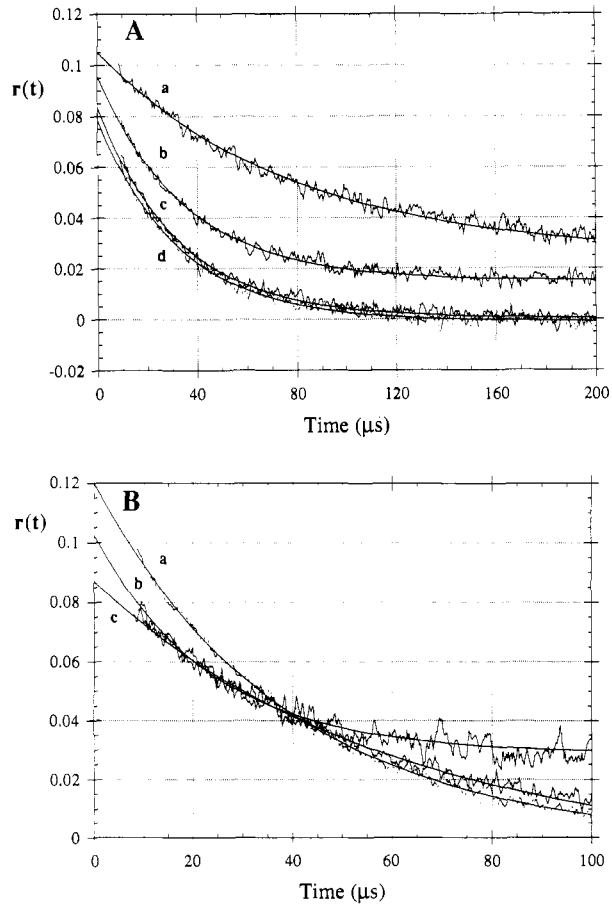


FIGURE 1: Decay of phosphorescence anisotropy of Er-labeled IgE and mAbs F4, H10, and J17 and their respective Fab fragments in ~70% aqueous sucrose solutions. (A) IgE (a) and mAbs H10 (b), J17 (c), and F4 (d) at 22 °C. (B) Fab fragments of J17 (a), H10 (b), and F4 (c) at 6–8 °C. The ligand concentrations were 10–30 nM. The smooth lines represent the fitted decay curves calculated with the parameters given in Table I.

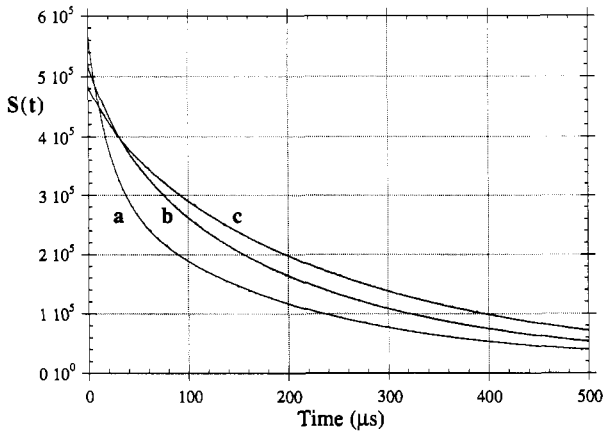


FIGURE 2: Phosphorescence intensity decay of Er-labeled IgE (a), mAb H10 (b), and the Fab fragment of mAb H10 (c) bound to the $Fc_\epsilon RI$ on RBL-2H3 cells at 4 °C. The original data are superimposed with the respective two-component fits. The lifetimes $\tau_i$(μs) and amplitudes (% in parentheses) are (a) 22 (48), 185 (52); (b) 39 (24), 206 (76); and (c) 34 (13), 248 (87). A complete set of three-component analyses is given in Table II.

agreed reasonably with those obtained from nanosecond decay of fluorescence anisotropy (Hanson et al., 1981; Oi et al., 1984), particularly considering the fact that the phosphorescence anisotropy decay measures the totality of the depolarization process. Thus, the longer range global motions are preferentially represented in the mean values of $\phi$.

A comparison of the calculated parameters of Er–IgE and of the Er–mAbs reveals interesting differences. Whereas both amplitudes and initial anisotropy values were quite similar, the normalized rotational correlation time of Er–IgE was ~3 times that of any of the Er–mAb conjugates. Part of the difference may have been due to the presence of IgE aggregates (see above). In addition, since the distinction in size between the IgG class mAbs and IgE is due to an additional ($C_\epsilon 4$) domain, a considerable slowing of rotation rate may be expected, particularly if the Er label is specifically situated on the monoclonal IgE such that it preferentially reports motions about the shorter axis of the molecule, i.e., tumbling. This rotational component is very sensitive to the maximal dimension of the molecule (Small & Isenberg, 1977).

*Monovalent Ligands Bound to $Fc_\epsilon RI$.* For the different ligands bound to RBL-2H3 cells, the emission was corrected for an apparent short-lived contribution from light scattering and intrinsic luminescence. This was achieved by subtraction of appropriate blank records obtained with unlabeled cells; the relative magnitude of the signals was generally < 3%. In Figure 2, the phosphorescence intensity decay kinetics are illustrated for the cell-bound Er–Fab fragment of the H10 mAb, as well as for the intact mAb and IgE. The time course of the phosphorescence decays, $S(t)$, was multiexponential, and the analyses of these and other data are summarized in Table II. The calculated triplet lifetime parameters are similar to those previously reported for other Er–antibody conjugates [see references in Table II in Jovin and Vaz (1989)].

The phosphorescence intensity and anisotropy of Er–IgE bound to RBL-2H3 cells were always examined as a reference in all experiments with the mAbs or their Fab fragments. The present Er–IgE decay patterns are similar to those observed earlier for both monoclonal rat (Zidovetzki et al., 1986b) and monoclonal murine (G. Barisas, I. Pecht, & T. M. Jovin, unpublished observations) IgE molecules. However, the signal-to-noise, blank suppression, and gating characteristics were significantly improved in the present version of the instrument so that a two-component analysis of the $r(t)$ curves could be carried out when required, as in the case of the cell-bound Er–IgE.

Table II: Phosphorescence Lifetimes of Er-Labeled $Fc_\epsilon RI$-Specific Monoclonal Antibodies and IgE Bound to RBL-2H3 Cells[a]

| probe | $T$ (°C) | $\tau_1$ (μs) | $\tau_2$ (μs) | $\tau_3$ (μs) |
|---|---|---|---|---|
| IgE | 5 | 15 (40) | 71 (25) | 286 (35) |
| | 15 | 8.7 (34) | 44 (27) | 203 (39) |
| | 25 | 5.4 (37) | 25 (36) | 115 (37) |
| | 35 | 5.5 (38) | 24 (32) | 94 (30) |
| H10 Fab | 5 | 24 (10) | 158 (37) | 361 (52) |
| | 15 | 85 (21) | 264 (79) | |
| | 25 | 22 (27) | 128 (56) | 259 (17) |
| | 35 | 18 (17) | 97 (42) | 118 (42) |
| J17 Fab | 5 | 44 (43) | 106 (27) | 269 (30) |
| | 15 | 27 (24) | 87 (37) | 269 (39) |
| | 25 | 11 (31) | 40 (32) | 160 (36) |
| | 35 | 6 (35) | 21 (34) | 87 (32) |
| F4 Fab | 6 | 23 (20) | 248 (80) | |
| | 15 | 20 (20) | 223 (80) | |
| | 24 | 13 (18) | 152 (82) | |
| H10 mAb | 5 | 20 (14) | 98 (36) | 301 (51) |
| | 15 | 19 (13) | 96 (31) | 313 (56) |
| | 25 | 17 (19) | 61 (25) | 206 (56) |
| | 35 | 17 (30) | 74 (35) | 137 (35) |
| J17 mAb | 5 | 76 (40) | 297 (60) | |
| | 15 | 5.7 (59) | 30 (21) | 209 (20) |
| | 25 | 8.6 (35) | 39 (30) | 171 (35) |
| | 35 | 5.3 (36) | 22 (31) | 109 (33) |
| F4 mAb | 5 | 8.7 (28) | 43 (25) | 229 (47) |
| | 15 | 8.5 (29) | 44 (27) | 219 (43) |
| | 25 | 4.9 (38) | 24 (26) | 130 (36) |
| | 35 | 5.0 (39) | 24 (29) | 113 (31) |

[a] The numbers in parentheses are fractional amplitudes (in %). In some fits, the base line (constant term in the exponential analysis) was fixed to 0.

The time-resolved anisotropy decay of the cell-bound Er–IgE and Er–Fab fragments at several temperatures is illustrated in Figure 3 and tabulated in Table III. The observed patterns are characteristic for membrane-associated macromolecules in that they display positive initial anisotropies, rotational correlation times in the range of 30–200 μs, and a nonzero limiting anisotropy. The $r_{in}$ values for the cell-bound Er–Fabs of F4 and H10 were in the range of 0.02–0.06 at 5 °C, and the corresponding $r_{in}$ for cell-bound Er–IgE was 0.07. The low $r_{in}$ values may be attributed to fast motion of the Er probe itself and some segmental motions of the IgE and Fabs occurring on a time scale faster than that detected by our system, as demonstrated by comparison with the anisotropy decay measurements in high-viscosity sucrose solutions. The cell-bound Er–Fab fragment of each individual mAb displayed distinct time-dependent anisotropy decay patterns. For both the F4 and H10 Fabs, the rotational correlation times extended from ~200 μs at 6 and 15 °C to ~30 μs at 25 and 35 °C. In addition, these two Er–Fabs had decays with positive amplitudes and initial values $r_{in}$ and finite (>0) plateau values (limiting anisotropy, $r_\infty$) in the same range as those for Er–IgE.

The time-dependent anisotropy of J17 Fab was more complex. At 5 °C a fast, very small positive decay phase was followed by a major component with a negative amplitude and an apparent $\phi$ of ~60 μs. At 15 °C practically no decay was evident, while raising the temperature further led to a decay with a positive amplitude and a rotational correlation time in the range of 50 μs. Depolarizations with negative amplitudes may appear unusual but can arise with nonspherical molecules undergoing anisotropic rotational motions such that the absorption and emission transition moments are brought into a more nearly parallel orientation during the excited-state lifetime [see eq 7c and associated text in Jovin and Vaz (1989)]. An example is provided by erythrosin labeled epi-

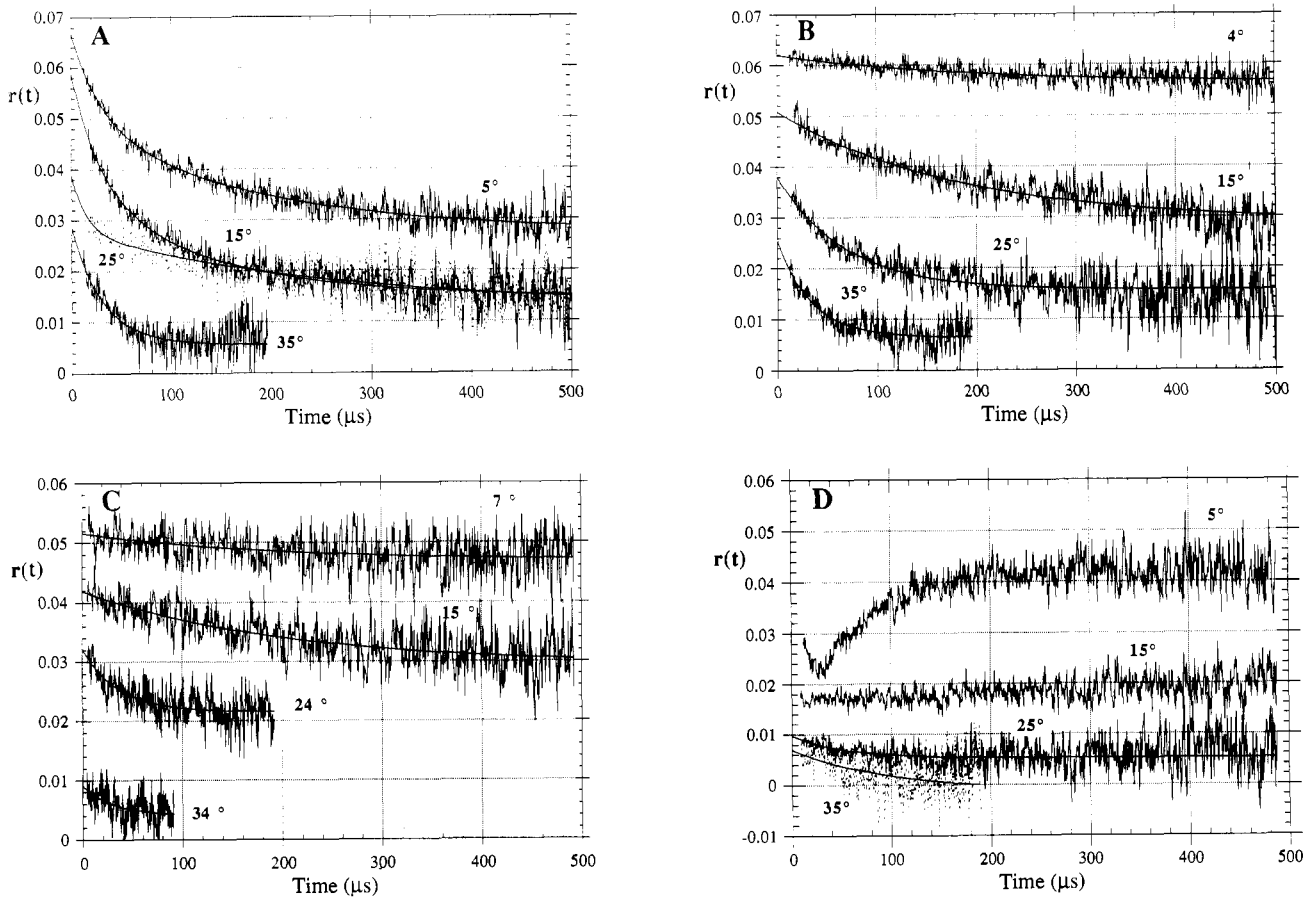


FIGURE 3: Anisotropy decay kinetics of Er-labeled IgE (A) and Fab fragments of the three $Fc_\epsilon RI$-specific mAbs H10 (B), F4 (C), and J17 (D) bound to RBL-2H3 cells and measured at the indicated temperatures. Cells were reacted with the different monovalent ligands as described under Materials and Methods, and measurements were performed at successively increasing temperatures. The smooth lines are the decay curves generated with the best fit parameters summarized in Table III.

dermal growth factor bound to its cellular receptor (Zidovetzki et al., 1981).

We demonstrated that the observed phosphorescence anisotropy decays were due to the specifically membrane-associated probes and that the Er–Fab fragments bind competitively to epitopes on the $Fc_\epsilon RI$ (Ortega et al., 1988) in experiments illustrated in Figure 4. Thus, the phosphorescence anisotropy of cell-bound Er–H10 Fab was reduced by ~80% as the result of incubation in the presence of an excess of unlabeled IgE for 2 h. Due to the low concentrations (nM) of $Fc_\epsilon RI$ sites available in the cell suspensions employed in these measurements, some dissociation of bound ligands would have taken place spontaneously during the course of several hours. The extent of dissociation was assessed in experiments in which cells were harvested and labeled by the routine protocol. After being washed, the cell samples were used for anisotropy measurements at 6 and 37 °C, and maintained at 0 °C for the intermittent periods. Four hours after the start of the experiments, the samples were centrifuged inside the cuvettes to sediment the cells and the phosphorescence intensity of the supernatants was measured at 6 °C. As expected for proteins in aqueous solution undergoing rapid rotation in the submicrosecond domain, the phosphorescence emission of the free antibodies was unpolarized. The fractional emission intensity of the supernatants, compared to the total initial values, varied among the mAbs employed. Whereas for Er–J17 (both intact and Fab fragment) about 28% of the phosphorescence intensity was found in the supernatant, only 5–9% of the Er–H10 dissociated. For the Er–F4 Fab, an intermediate value of 14% of the phosphorescence signal remained in the supernatant but increased to 57% at 34 °C (Table III). Although the estimates of dissociation are exaggerated because the clear supernatants do not experience the same degree of signal loss due to scattering as do the original cell suspensions, the results are in accordance with the relative binding affinities (Ortega et al., 1988) and interaction kinetics (E. Ortega, R. Schweitzer-Stenner, and I. Pecht, unpublished data) of the three Fabs. Thus, the F4 and J17 Fabs have a lower affinity than H10 and IgE and dissociate faster, particularly at higher

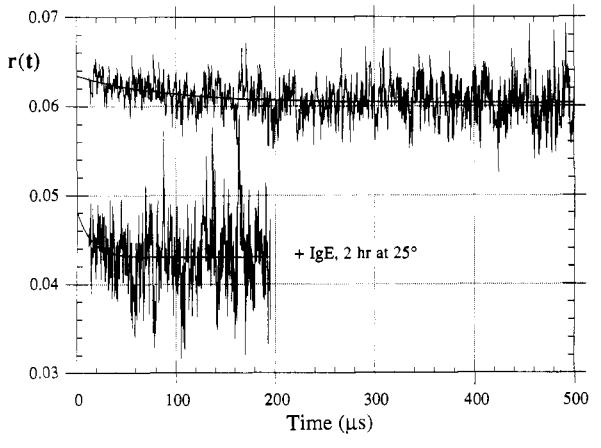


FIGURE 4: Displacement of Er-labeled H10 Fab bound to RBL-2H3 cells by unlabeled IgE. In the upper trace is the anisotropy decay of a sample of cell-bound Er–Fab of H10 prepared and measured at 5 °C as in Figure 3B. To this sample was added unlabeled monoclonal IgE to a concentration of 1 μM. After incubation for 2 h at 25 °C, the anisotropy was remeasured at 5 °C (lower trace).

Table III: Phosphorescence Anisotropy Decay Parameters of $Fc_\epsilon RI$-Specific Probes Bound to RBL-2H3 Cells[a]

| ligand | $T$ (°C) | $\phi$ (μs) | $\alpha$ | $r_\infty$ | $r_{in}$ | $r_\infty/r_{in}$ |
|---|---|---|---|---|---|---|
| IgE | 5 | 30/186 | 0.018/0.022 | 0.027 | 0.067 | 0.40 |
| | 15 | 29/134 | 0.022/0.022 | 0.015 | 0.059 | 0.25 |
| | 25 | 14/267 | 0.011/0.015 | 0.012 | 0.039 | 0.31 |
| | 35 | 30 | 0.023 | 0.006 | 0.029 | |
| H10 Fab | 5 | 199 | 0.005 | 0.056 | 0.062 | 0.90 |
| | 15[b] | 184 | 0.022 | 0.028 | 0.051 | 0.55 |
| | 25 | 68 | 0.022 | 0.016 | 0.038 | 0.42 |
| | 35 | 34 | 0.019 | 0.006 | 0.025 | 0.24 |
| J17 Fab | 5[c] | 63 | −0.032 | 0.042 | ~0.03 | ~1.4 |
| | 15 | | <0.004 | | 0.017 | |
| | 25 | | <0.004 | | 0.010 | |
| | 35 | 100 | 0.008 | −0.001 | 0.007 | |
| F4 Fab | 7 | 189 | 0.005 | 0.056 | 0.062 | 0.90 |
| | 18 | 210 | 0.022 | 0.028 | 0.050 | 0.56 |
| | 24 | 36 | 0.011 | 0.010 | 0.021 | 0.48 |
| | 34[d] | 31 | 0.005 | 0.004 | 0.009 | |
| H10 mAb | 5 | 80 | 0.007 | 0.034 | 0.041 | 0.83 |
| | 15 | 71[e] | 0.015 | 0.020 | 0.035 | 0.57 |
| | 25 | 76 | 0.016 | 0.012 | 0.027 | 0.44 |
| | 35 | 37 | 0.014 | 0.009 | 0.022 | 0.41 |
| J17 mAb | 5 | | <0.004 | | 0.029 | |
| | 15 | | <0.004 | | 0.024 | |
| | 25 | | <0.004 | | 0.019 | |
| | 35 | 124 | 0.013 | 0.001 | 0.014 | |
| F4 mAb | 5 | | <0.004 | | 0.045 | |
| | 15 | | <0.004 | | 0.042 | |
| | 25 | | <0.004 | | 0.042 | |
| | 35 | | <0.004 | | 0.036 | |

[a] Decay curves are depicted in Figures 3 (IgE and Fabs) and 6 (mAbs). Files were averaged as in Table I. No values of $\phi$ are given for curves with amplitude changes <0.004. Two-component analyses are indicated by values separated by a slash. [b] Individual analyses of four records yielded ranges for values of $\phi$, $\alpha$, and $r_{in}$ (expressed as percentages of the means) of 38, 14, and 6, respectively. [c] One-component analysis for data >35 μs corresponding to the slow-rising phase. [d] Centrifugation of the sample yielded 57% of the phosphorescence signal (depolarized) in the supernatant. [e] This value was recorded 12 min after transfer from 5 to 15 °C. At 5 and 8.5 min, $\phi$ was 116 and 99 μs, respectively. The curve shown in Figure 6A is an average of the three records with a $\phi$ of 90 μs.

temperatures. One should note that the measured population averages of $r_{in}$, $\alpha$, and $r_\infty$ for the cell suspensions will be reduced in magnitude in proportion to the extent of ligand dissociation but that the values of $\phi$ remain unaffected.

The similarities and differences in the anisotropy decay behavior of Er–IgE and the three Er–Fab fragments, all ligands that bind monovalently to the $Fc_\epsilon RI$, merit further discussion. For exmple, at temperatures <25 °C, the IgE and the F4 and H10 Fab probes exhibited long rotational correlation times (130–210 μs) and $r_{in}$ values in the range 0.05–0.07. However, the rotational depolarization of the bound IgE had a second faster component accounting for approximately half of the total amplitude, suggesting that, in addition to the inherent dynamics of the $Fc_\epsilon RI$, some contribution from wobbling or segmental motions of the IgE molecule distal to the $Fc_\epsilon RI$-binding domain may occur in the microsecond time domain. Such a property is not generally ascribed to proteins in an aqueous environment, but its existence would be consistent with a recent study of the flexibility in the nanosecond range displayed by IgE bound to $Fc_\epsilon RI$ in membrane vesicles where evidence for microsecond depolarizations was reported (Holowka et al., 1990). We would not expect to perceive such slow molecular flexion in homogeneous high viscosity solutions (70% sucrose) because under this condition the global rotational depolarization of the IgE molecule (in this case untethered) dominates the decay kinetics. If one assumes further that the Er is conjugated mainly to the Fab domains of the IgE (Holowka & Baird, 1983), the probe should exhibit greater motional freedom than the bound Fc domains, or the Fab fragments of the $Fc_\epsilon RI$-specific mAbs. The latter ligands, being smaller and bound via their respective variable domains, are likely to be more constrained with respect to internal motions and hence report more directly the rotation of the $Fc_\epsilon RI$ itself and the specific antigenic epitopes. [One must keep in mind that the single measured rotational correlation time represents a weighted mean of all components contributing to depolarization in the time range examined (Jovin & Vaz, 1989). It therefore reflects the temperature dependence of the preexponential terms as well as of the $\phi s$ (diffusion constants) themselves.]

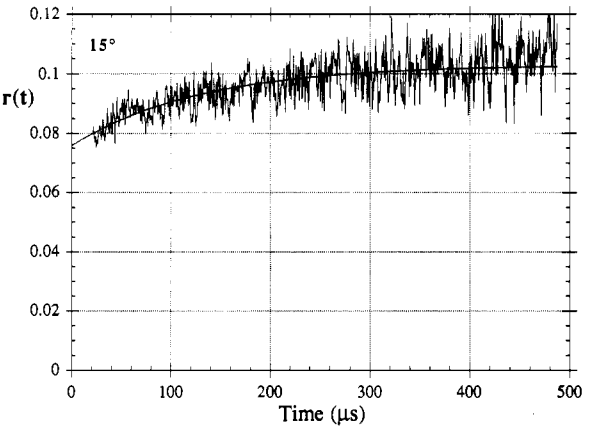


FIGURE 5: Phosphorescence anisotropy decay of Er-labeled, DNP-specific, monoclonal IgE bound to DNP-Sepharose 4B. Er–IgE was reacted for 1 h with the Sepharose beads, which were then washed and resuspended in buffer for anisotropy measurements at 16 °C. The apparent $\phi$ is 130 μs.

These interpretations are further supported by results of another experiment in which the DNP-specific monoclonal IgE (Er labeled) was bound to DNP-derivatized Sepharose beads. Following incubation for 60 min and repeated washings, the beads carrying Er–IgE were suspended in buffer, and the emission anisotropy was measured as for the cell-bound ligands. The results demonstrated a pronounced degree of immobilization of the bound Er–IgE (Figure 5). Thus, at both

16 and 25 °C the anisotropy increased to ~0.09–0.10 from the already high $r_{in}$ of ~0.06, a value similar to that for cell-bound IgE at 15 °C. After sedimentation of the beads by centrifugation, the supernatants had a residual phosphorescence of ~15% of the initial value and no detectable anisotropy. The $r_{in}$ of the tethered Er–IgE was also similar to that of Er–DNP-lysine bound to the combining site of the DNP-specific IgE measured in viscous glycerol solutions (G. Barisas, I. Pecht, and T. M. Jovin, unpublished data). We do not attempt a more quantitative assessment of these experiments because such a system is clearly heterogeneous with respect to the DNP attachment sites on the matrix and the mode of IgE binding, which is potentially both monopedal and bipedal. However, the results strongly suggest that tethering the Er–IgE via its Fab domains eliminates a major component of the rotational depolarization observed in the Er–IgE bound to cells via its other ($Fc_\epsilon$) end.

The marked differences observed among the cell-bound Er–Fabs, in terms of both the amplitudes and time dependence of the anisotropy decay, probably reflect nonrandom orientation of these probes relative to the cell membrane, and thus to the uniaxial or more complex axes of rotation of the $Fc_\epsilon RI$. As reported elsewhere (Ortega et al., 1988), the observed mutual displacement of these mAbs and of IgE from $Fc_\epsilon RI$ suggests that the binding epitopes of all three $Fc_\epsilon RI$-specific mAbs and the $Fc_\epsilon$-binding site must lie in molecular proximity, i.e., within a radius of ca. 3–4 nm. However, they are not identical, inasmuch as the respective affinities, rates of association and dissociation, and the extent of induced secretion are quite different. That is, we may conclude that the dynamics of the $Fc_\epsilon$-binding site and the mAb-binding epitopes on the $Fc_\epsilon RI$ are specific and relatively autonomous.

This conclusion may be rationalized as follows in the case of the $Fc_\epsilon RI$-bound Er–Fab fragments. Since on the average <2 Er molecules were conjugated per Fab fragment, it is probable that the spatial distribution of the attachment sites on the protein surface was relatively limited. Furthermore, although the Fabs bind to epitopes that are close to each other, their orientation in the bound state with respect to the membrane surface is in principle fixed but arbitrary. That the dispositions of the various Er–Fabs differ is further indicated by the changes observed in $r_\infty/r_{in}$ values with increasing temperature. This ratio remains approximately constant (Zidovetzki et al., 1986b) or decreases slightly (this study) in the case of cell-bound Er–IgE. A more dramatic decrease was observed for both the F4 and H10 Er–Fabs. The quantity $r_\infty/r_{in}$ has been shown to be a measure of the distribution width of a probe's transition moments around the membrane's normal and had been termed the "degree of orientational constraints" (Kinosita et al., 1977, 1984; Szabo, 1984; Jovin & Vaz, 1989). The long rotational correlation times at low temperature, particularly when associated with low amplitudes, are difficult to interpret unambiguously. From the photophysical standpoint [see discussion in Jovin and Vaz (1989)], one has to consider the possible contributions of overlapping and compensating components, heterogeneity with respect to $\tau_i$ and $\phi_i$ values, and unique orientations of transition moments leading to an observed $r(t)$ that may not reflect the true rotational dynamics of the system. However, the data may simply indicate that the $Fc_\epsilon RI$, or more precisely, particular ligand–receptor complexes, may be relatively immobile at <25 °C. [One possibility proposed by a reviewer of the manuscript was that the Er moiety or the protein ligand may be experiencing "drag" due to interactions with membrane components in the environment of the $Fc_\epsilon RI$.] In view of these considerations,

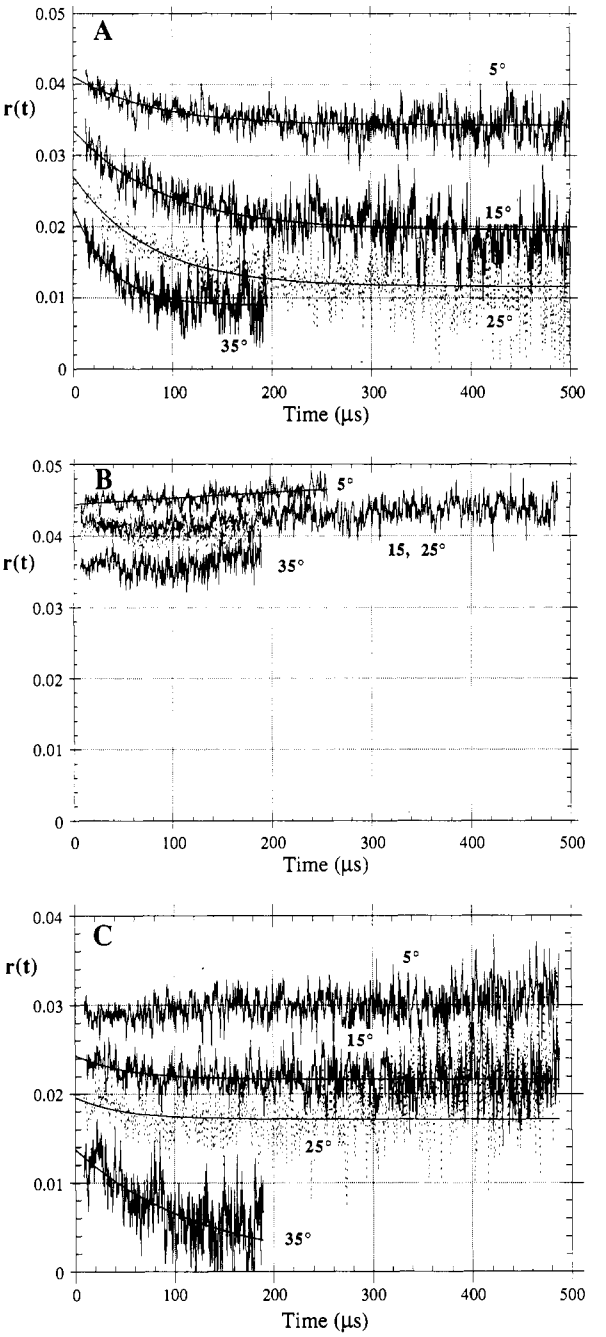


FIGURE 6: Phosphorescence anisotropy decay kinetics of Er-labeled intact $Fc_\epsilon RI$-specific mAbs bound to RBL-2H3 cells. Labeled cell samples were prepared as described under Materials and Methods and were measured at successively increasing temperatures. (A) H10 (see footnote to Table III); (B) F4; (C) J17.

it is very significant that the rotational correlation times practically converged at higher temperatures ($\phi$ = 30–40 μs). One is led to conclude that the rotational dynamics deduced from experiments probing the $Fc_\epsilon RI$ with different reagents reflect both features of the Er-attachment site and other domains of the protein, as well as the properties of the cell surface receptor. At the physiological temperature, certain constraints are relieved and the $Fc_\epsilon RI$ dynamics dominate the observed behavior.

*Binding of Intact mAbs to the $Fc_\epsilon RI$.* Distinct time-resolved phosphorescence anisotropy decay patterns were observed for each of the three $Fc_\epsilon RI$-specific intact mAbs bound to RBL-2H3 cells (Figure 6; Table III). The initial anisotropies of all three mAbs were in the range 0.03–0.5 at low temperature and decreased considerably with rising temperature (Figure

6). The Er conjugate of the H10 mAb was the only one that exhibits a positive amplitude over the entire temperature range examined. The corresponding rotational correlation times were surprisingly short, lower even than that of the H10 Fab at 5 °C and dropping to a value very similar to that for the monovalent ligands (except for the J17 Fab) at the highest temperature. In contrast, the Er–J17 mAb showed a small, fast, positive component followed by a slow phase ($\phi = \sim 100$ μs) with a small negative amplitude at 5 °C. Raising the temperature led to the appearance of a single positive amplitude decay component. These characteristics of the phosphorescence anisotropy of the J17 mAb bound to the $Fc_\epsilon RI$ resemble those of its Fab fragment, supporting the contention that probe conjugation and orientation were relatively specific. The Er–F4 mAb was unique in that it showed a practically constant phosphorescence anisotropy at all temperatures. Whereas we cannot formally exclude the temporal superposition of positive and negative components as the source of apparent immobilization, it seems unlikely that such a circumstance would hold from 5 to 35 °C.

The time course of phosphorescence anisotropy, particularly in the case of the F4 mAb, appears to reflect a degree of immobilization which is greater than that expected merely from the formation of $Fc_\epsilon RI$ dimers and could be interpreted as evidence that higher order oligomers arise following the initial nucleation by dimer formation. Evidence for such a nucleating role of small $Fc_\epsilon RI$ oligomers has emerged from the studies of Holowka and Baird with their associates (Menon et al., 1986a,b; Robertson et al., 1986). All these observations are consistent with the simplest general model (Balakrishnan et al., 1982; Pecht et al., 1989) that assumes the existence in the cell membrane of a preequilibrium between monomeric $Fc_\epsilon RI$ and specific molecular complexes of the receptors. In the resting state, the concentration of such complexes of $Fc_\epsilon RI$ is too low to yield any significant secretion. Receptor cross-linking would be one pathway to displace the equilibrium, thereby increasing the concentration of specific molecular complexes required to initiate the cellular response. The clear differences in the anisotropy decay patterns of the three cell-bound Er–mAbs examined may reflect possible differences in the efficiency with which they can displace the preequilibrium state. Particularly noteworthy in this connection is the correlation between the extent of immobilization monitored in the present measurements of the $Fc_\epsilon RI$ bound mAbs and their capacity for inducing secretion. Thus, while the H10 mAb (as well as its Fab) has by far the highest affinity from equilibrium measurements (Ortega et al., 1988), it exhibits the highest rotational mobility and is least effective in inducing secretion. In contrast, the F4 mAb has a much lower affinity yet is apparently immobile in the bound state and evokes the maximal cellular response. Furthermore, the rotational correlation times for the H10 mAb are less than or equal to to those of its corresponding Fab fragment. One possible interpretation reconciling these observations would state that (i) the F4 and J17 mAbs bind bipedally to a significant degree, i.e., cross-link two neighboring $Fc_\epsilon RI$ to a degree so as to form a dimeric species, whereas (ii) a significant fraction of the bound H10 mAb is monopedal during the triplet lifetime defining the temporal window of the rotational depolarization experiment. Such an explanation would be compatible with the inability to fit the H10 mAb-binding data at 37 °C with a model assuming the same high intrinsic affinity constant as that of the corresponding Fab (Ortega et al., 1988). Possibly, the intact antibody is sterically hindered in its interactions with the epitope such that rapid flip-flop association–dissociation events involving one of the two Fab domains occur, a mechanism that would not be in contradiction to the observed dimer stoichiometry. Alternatively, the H10 mAb may be so disposed that the two Fab domains can experience independent rapid motions leading to the perceived depolarization. Either model would be consistent with the notion that the $Fc_\epsilon RI$ dimer must achieve a rather specific, relatively rigid stereochemical orientation in order to be biologically active in the initiation of the cascade leading to exocytosis.

It is worthwhile to compare the present results with earlier data on the effect of cross-linking $Fc_\epsilon RI$–IgE complexes by polyclonal anti-IgE antibodies (Zidovetzki et al., 1986b). In that study, immobilization of Er–IgE was practically complete such that no anisotropy decay could be resolved in the time domain examined, even at 37 °C. Moreover, the observed anisotropy was considerably higher (0.06) than that induced upon Er–F4 cross-linking of the $Fc_\epsilon RI$ (~0.04, Table III). The different behavior most probably reflects the more extensive cross-linking and hence immobilization induced by the polyclonal anti-IgE antibodies. More recent studies using a monoclonal anti-IgE antibody to cross-link $Fc_\epsilon RI$–IgE complexes are consistent with this interpretation (E. Ortega, I. Pecht, and T. M. Jovin, unpublished data).

*Concluding Remarks.* The data presented here demonstrate that molecular properties of specific macromolecular ligands bound to cell-surface receptors can be assessed by direct spectroscopic means. As a consequence, it is possible to monitor the basic distinctions between monomeric and polyvalent ligands for cell plasma membrane components. The monovalent ligands that we have used (Fabs of $Fc_\epsilon RI$-specific mAbs and the natural ligand IgE) reflect the properties of the individual receptor–ligand complexes. However, the polyvalent ligands (intact mAbs, allergens, or anti–IgE antibodies) promote interactions between receptors with physical and functional consequences that can vary considerably. Thus, although the F4 antibody binds with much lower affinity than H10, its complex with the $Fc_\epsilon RI$ displays greater rigidity as measured by the phosphorescence anisotropy technique. One can speculate whether the apparent rigidity of the bound F4 is correlated with its superior triggering of exocytosis. The differential propensity of dimerized receptors to propagate into immobile species may be a significant factor in this respect. In any event, it would appear that the rather asymmetric molecular assembly constituting the $Fc_\epsilon RI$ comprises domains differing in flexibility and/or dynamics. These features may well be general to other equally complex cell-surface components involved in signal transduction.

## Acknowledgments

We gratefully acknowledge the continuous devoted help and advice of Dr. Donna Arndt-Jovin and the preparation and characterization of several reagents by Mr. Arieh Licht. We are indebted to Drs. I. Z. Steinberg, G. Barisas, and L. Trŏn for critical reading of the manuscript.

## References

Balakrishnan, K., Hsu, F. J., Cooper, A. D., & McConnell, H. M. (1982) *J. Biol. Chem. 257*, 6427.

Blank, U., Ra, C., Miller, L., White, H., Metzger, H., & Kinet, J. P. (1989) *Nature 337*, 187.

DeLisi, C. (1979) in *Physical Chemical Aspects of Cell Surface Events in Cellular Regulation* (DeLisi, C., & Blumenthal, R., Eds.) pp 261–292, Elsevier, New York.

DeLisi, C. (1981) *Nature 289*, 322.

Edidin, M. (1987) *Curr. Top. Membr. Transp. 39*, 91.

Froese, A. (1984) *Prog. Allergy 34*, 142.

Goetzl, E. J., & Metzger, H. (1970) *Biochemistry 9*, 1267.
Helm, B., Marsh, P., Vercelli, D., Padlan, E., Gould, H., & Geha, R. (1988) *Nature 331*, 181.
Henson, D. C., Yguerabide, J., & Schumaker, V. N. (1981) *Biochemistry 20*, 6842.
Holowka, D., & Baird, B. (1983) *Biochemistry 22*, 3475.
Holowka, D., Wensel, T., & Baird, B. (1990) *Biochemistry 29*, 4607.
Ishizaka, T., & Ishizaka, K. (1984) *Prog. Allergy* 34, 188.
Jovin, T. M., & Vaz, W. (1989) *Methods Enzymol. 172*, 471.
Kaganov, I. N. (1982) *Sakh. Promst. 8*, 57.
Kinet, J. P. (1989) *Cell 57*, 351.
Kinosita, K., Jr., Kawato, S., & Ikegami, A. (1977) *Biophys. J. 20*, 289.
Kinosita, K., Jr., Kawato, S., & Ikegami, A. (1984) *Adv. Biophys. 17*, 147.
Lipari, G., & Szabo, A. (1980) *Biophys. J. 30*, 489.
Liu, F. T., Bohn, J. W., Ferry, E. L., Yamamoto, H., Molinaro, C. A., Sherman, L. A., Klinman, N. R., Katz, D. H. (1980) *J. Immunol. 124*, 2728.
Matayoshi, E. D., Corin, A. F., Zidovetzki, R., Sawyer, D. H., & Jovin, T. M. (1983) in *Mobility and Recognition in Cell Biology* (Sund, H., & Veeger, C., Eds.) pp 119-134, de Gruyter, Berlin.
McCloskey, M. A., Liu, Z.-Y., & Poo, M.-M (1984) *J. Cell Biol. 99*, 778.
Menon, A. K., Holowka, D., Webb, W. W., & Baird B. (1986a) *J. Cell Biol. 102*, 534.
Menon, A. K., Holowka, D., Webb, W. W., & Baird, B. (1986b) *J. Cell Biol. 102*, 541.
Metzger, H., Alcaraz, G., Hohman, R., Kinet, J. P., Pribluda, K., & Quarto, R. (1986) *Annu. Rev. Immunol. 4*, 419.
Oi, V. T., Vuong, T. M., Hardy, R., Reidler, J., Dangl, J., Herzenberg, L. A., & Stryer, L. (1984) *Nature 307*, 136.
Ortega, E., Schweitzer-Stenner, R., & Pecht, I. (1988) *EMBO J. 7*, 4101.
Ortega, E., Schweitzer-Stenner, R., & Pecht, I. (1990) *Biophys. J. 57*, 284a.
Pecht, I., Schweitzer-Stenner, R., & Ortega, E. (1989) *Prog. Immunol. 7*, 676.
Rivnay, B., Wank, S. A., & Metzger, H. (1982) *Biochemistry 21*, 6922.
Robertson, D., Holowka, D., & Baird, B. (1986) *J. Immunol. 136*, 4565.
Schwarzbaum, S., Nissim, A., Alkalay, I., Ghozi, M. C., Schindler, D. G., Bergman, Y., & Eshhar, Z. (1989) *Eur. J. Immunol. 19*, 1015.
Siraganian, R. P. (1988) in *Inflammation: Basic Principles and Clinical Correlates* (Gallin, J. I., Goldstein, I. M., & Snyderman R., Eds.) pp 513-542, Raven Press, New York.
Small, E. W., & Isenberg, I. (1977) *Biopolymers 16*, 1907.
Szabo, A. (1984) *J. Chem. Phys. 81*, 150.
Yashida, T. M., Jovin, T. M., & Barisas, G. (1989) *Rev. Sci. Instrum. 60*, 29.
Zidovetzki, R., Yarden, Y., Schlessinger, J., & Jovin, T. M. (1981) *Proc. Natl. Acad. Sci. U.S.A. 78*, 6981.
Zidovetzki, R., Yarden, Y., Schlessinger, J., & Jovin, T. M. (1986a) *EMBO J. 5*, 247.
Zidovetzki, R., Bartholdi, M., Arndt-Jovin, D., & Jovin, T. M. (1986b) *Biochemistry 25*, 4397.

# Epimerization of D-Glucose to L-Galactose during the Biosynthesis of a Sulfated L-Galactan in the Ascidian Tunic†

Paulo A. S. Mourão

*Departamento de Bioquímica, Centro de Ciências da Saúde, Universidade Federal do Rio de Janeiro, Caixa Postal 68041, Rio de Janeiro, RJ 21910, Brazil*

*Received September 4, 1990; Revised Manuscript Received November 1, 1990*

ABSTRACT: The sulfated polysaccharides occurring in the tunic of ascidians are unique among known sulfated polysaccharides in that their major constituent sugar is galactose, which occurs exclusively in the L-enantiomeric form. In vitro incorporation experiments using tunic slices incubated with $^{14}C$-labeled sugars revealed that cells from this tissue epimerize D-isomers of hexose into L-galactose during the biosynthesis of their constituent polysaccharides. Compared with other hexoses, the precursor D-[$^{14}C$]glucose has the highest rate of incorporation and produces the highest proportion of L-galactose units. This metabolic pathway is distinct from the epimerization of D-mannose to L-galactose through its guanosine 5'-diphosphate nucleotide, described previously in an alga and in a snail. Therefore, the epimerization of D-glucose to L-galactose in the ascidian tunic occurs through a novel metabolic route, which involves inversion of the configuration of carbon atoms 2, 3, and 5 of the hexosyl moieties.

Sulfated polysaccharides are widespread in nature, occurring in a great variety of organisms. In marine algae, for example, the carrageenans and fucoidans are composed mainly of sulfated galactose and sulfated fucose, respectively (Painter, 1983). In the animal kingdom, sulfated glycosaminoglycans abound in vertebrate connective tissues (Mathews, 1975) and, in smaller quantities, are also present in invertebrates (Mathews, 1975; Cássaro & Dietrich, 1977).

In previous studies we have reported the isolation of novel sulfated polysaccharides from invertebrate tissues: the tunic of ascidians (Albano & Mourão, 1983, 1986; Mourão &

† This work was supported by grants from Conselho Nacional de Desenvolvimento Científico e Tecnológico (CNPq), Fundação Banco do Brasil, Fundação de Amparo à Pesquisa do Estado do Rio de Janeiro (FAPERJ), and Financiadora de Estudos e Projetos (FINEP).

0006-2960/91/0430-3458$02.50/0 